

## RESEARCH OUTPUTS / RÉSULTATS DE RECHERCHE

### Diffractionnelle hygrochromique effect in the cuticle of the hercules beetle *Dynastes hercules*

Rassart, Marie; Colomer, Jean-François; Tabarrant, Tijani; Vigneron, Jean-Pol

*Published in:*  
New Journal of Physics

*Publication date:*  
2008

#### [Link to publication](#)

*Citation for published version (HARVARD):*

Rassart, M, Colomer, J-F, Tabarrant, T & Vigneron, J-P 2008, 'Diffractionnelle hygrochromique effect in the cuticle of the hercules beetle *Dynastes hercules*', *New Journal of Physics*, vol. 10, no. 033014, pp. 1-14.  
<[http://www.iop.org/EJ/article/1367-2630/10/3/033014/njp8\\_3\\_033014.html](http://www.iop.org/EJ/article/1367-2630/10/3/033014/njp8_3_033014.html)>

#### General rights

Copyright and moral rights for the publications made accessible in the public portal are retained by the authors and/or other copyright owners and it is a condition of accessing publications that users recognise and abide by the legal requirements associated with these rights.

- Users may download and print one copy of any publication from the public portal for the purpose of private study or research.
- You may not further distribute the material or use it for any profit-making activity or commercial gain
- You may freely distribute the URL identifying the publication in the public portal ?

#### Take down policy

If you believe that this document breaches copyright please contact us providing details, and we will remove access to the work immediately and investigate your claim.

## Diffractional hydrochromic effect in the cuticle of the hercules beetle *Dynastes hercules*

This article has been downloaded from IOPscience. Please scroll down to see the full text article.

2008 New J. Phys. 10 033014

(<http://iopscience.iop.org/1367-2630/10/3/033014>)

View [the table of contents for this issue](#), or go to the [journal homepage](#) for more

Download details:

IP Address: 138.48.4.247

The article was downloaded on 04/11/2012 at 12:16

Please note that [terms and conditions apply](#).

## Diffractional hygrochromic effect in the cuticle of the hercules beetle *Dynastes hercules*

M Rassart<sup>1,3</sup>, J-F Colomer<sup>1</sup>, T Tabarrant<sup>2</sup> and J P Vigneron<sup>1</sup>

<sup>1</sup> Laboratoire de Physique du Solide, University of Namur, 61 rue de Bruxelles, 5000 Namur, Belgium

<sup>2</sup> Laboratoire de Physique des Matériaux Electroniques, University of Namur, 61 rue de Bruxelles, 5000 Namur, Belgium

E-mail: [marie.rassart@fundp.ac.be](mailto:marie.rassart@fundp.ac.be)

*New Journal of Physics* **10** (2008) 033014 (14pp)

Received 14 January 2008

Published 11 March 2008

Online at <http://www.njp.org/>

doi:10.1088/1367-2630/10/3/033014

**Abstract.** The elytra from dry specimens of the hercules beetle, *Dynastes hercules* appear khaki-green in a dry atmosphere and turn black passively under high humidity levels. New scanning electron images, spectrophotometric measurements and physical modelling are used to unveil the mechanism of this colouration switch. The visible dry-state greenish colouration originates from a widely open porous layer located 3  $\mu\text{m}$  below the cuticle surface. The structure of this layer is three-dimensional, with a network of filamentary strings, arranged in layers parallel to the cuticle surface and stiffening an array of strong cylindrical pillars oriented normal to the surface. Unexpectedly, diffraction plays a significant role in the broadband colouration of the cuticle in the dry state. The backscattering caused by this layer disappears when water infiltrates the structure and weakens the refractive index differences.

<sup>3</sup> Author to whom any correspondence should be addressed.

**Contents**

<b>1. Introduction</b>	<b>2</b>
<b>2. Spectral analysis of both states of <i>Dynastes hercules</i></b>	<b>5</b>
<b>3. Scanning electron microscope images of the cuticle</b>	<b>7</b>
<b>4. Modelling the hygrochromic structure</b>	<b>8</b>
4.1. Simplified model . . . . .	8
4.2. Optical response of a 3D model structure . . . . .	9
<b>5. Conclusion</b>	<b>12</b>
<b>Acknowledgments</b>	<b>12</b>
<b>Appendix</b>	<b>13</b>
<b>References</b>	<b>13</b>

**1. Introduction**

Nature supports at least two types of colouration mechanisms: selective absorption by pigments and interferential light filtering by transparent inhomogeneous media. In the so-called pigmentary mechanism, very common with living organisms, the scattering spectrum is modulated by the excitation of electronic standing waves in dye molecules, while in the light interference mechanism, the re-radiated spectrum is directly shaped by photon standing waves in much larger structures. The latter mechanism requires the propagation of light in weakly absorbing structures, such as multilayers, which produce interference after multiple reflections, or gratings, which produce diffraction. In rarer cases, both effects combine when light encounters more general three-dimensional (3D) structures—termed, when periodic, ‘photonic crystals’—which combine refractive index variations in two or three space dimensions.

Colouration by interference, also referred to as *structural* colouration, has been known to occur in living organisms for quite a long time [1]–[11] and biologists have given sustained attention to this subject throughout this time, including very recent years. Physicists have renewed some interest for the study of these natural photonic structures much more recently [12]–[14], mainly because these media happened to be very interesting examples of optical metamaterials, that draw their optical properties from highly-tunable submicron geometric shapes, rather than from the nature of the materials used to make them. These complex structures, found on many living species: birds, insects, snakes, fish and even mammals [15], could be a very effective and inspirational track to new visual effects or even new optical devices [16].

The structure described in the present study is very special, because its optical response can be drastically changed by its exposure to humidity. This phenomenon is one of the astonishing characteristics of a tropical beetle, *Dynastes hercules* (see figure 1). This visual effect was first described and examined by Hinton and Jarman [17], who found its origin in a porous structure made of chitin and air, organized with refractive index variations normal to the cuticle surface, in a way essentially analogous to a simple multilayer stack. This organization led to the assumption that the colouration could be explained by a porous multilayer with a reflectance that could be controlled by flooding the layer with liquid water. However, this interpretation still needs to be



**Figure 1.** The hercules beetle *Dynastes hercules* shows a greenish colouration with black spots. Some specimens may not present these black spots.

confirmed by a deeper physical analysis, measuring optical reflectance spectra and comparing them with detailed numerical simulations of the optical response of the structure.

The distance between an ideal multilayer response and the actual visual effect produced by the surface of the beetle's elytra is visible by the naked eye. A multilayer stack generally produces a bright metallic-like colour by multiple interferences and usually shows iridescence [18], as the dominant reflected colour is blue-shifted when the angle of incidence increases. This is not observed here, but it is known that structural iridescence can sometimes be avoided by special choices of the multilayer parameters [19, 20] or by the introduction of a sufficient level of disorder [21].

The insect studied here is sometimes called a 'rhinoceros beetle' because males have a long appendix, resembling a horn, which can be even longer than the rest of the body. The hercules beetle is known as one of the largest Coleoptera: it can in exceptional cases reach 170 mm in length. It seems also to be the strongest creature on earth as it is able to carry 850 times its own body weight. The larva which, in its final stage, measures 110 mm and weighs some 120 g, feeds on rotten wood during two years. Then it transforms into a pupa and later to the adult form. The adult *Dynastes hercules* feeds on rotten fruit on the floor of the mesohydrophilic (meaning the ground is always moist) forests of Central America, North of South America and the Antilles [22, 23]. The subspecies *lichyi* (Lachaume, 1985) under specific study here can be found in Columbia, Venezuela, Peru, Ecuador, Bolivia and Brazil. Each subspecies [24] has indeed its own area distribution (see figure 2), the geographical isolation being one of the criterions of the definition of a subspecies.

The greenish colour of the *Dynastes hercules* turns to black as water penetrates the multilayer (see figure 3). The beetle looks totally dark under very humid conditions (more than 80% humidity [17]). Only a few insects are known to change their colouration reversibly by modifying the level of hydration of their elytra: some of the most spectacular species belong to the Cassidinae family [25] and undergo active colouration changes when the insect get stressed.

The biological and evolutive advantage that drove the development of this capability is not known. Hinton and Jarman [26] speculated that, under tropical climates, the humidity level increases at night and the beetle becomes black, reaching a better state of camouflage at the time the imago insect is most active. During the day when the humidity level decreases, its greenish colouration better matches its tropical coloured environment. However this camouflage

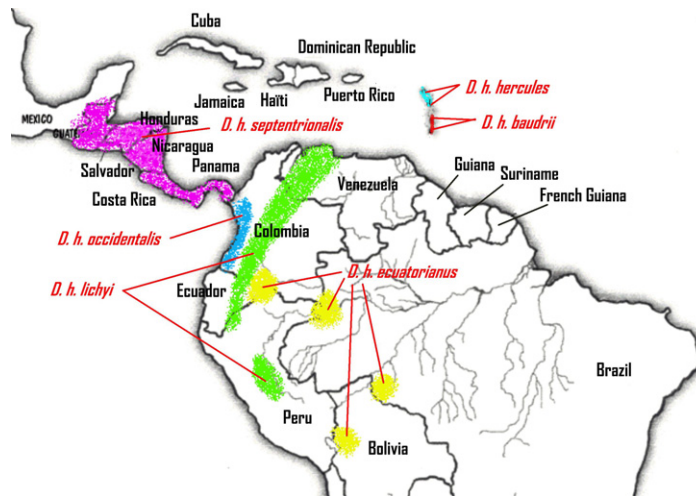


**Figure 2.** Geographical distribution of some subspecies of *Dynastes hercules* including *Dynastes hercules lichyi* (from [22]).

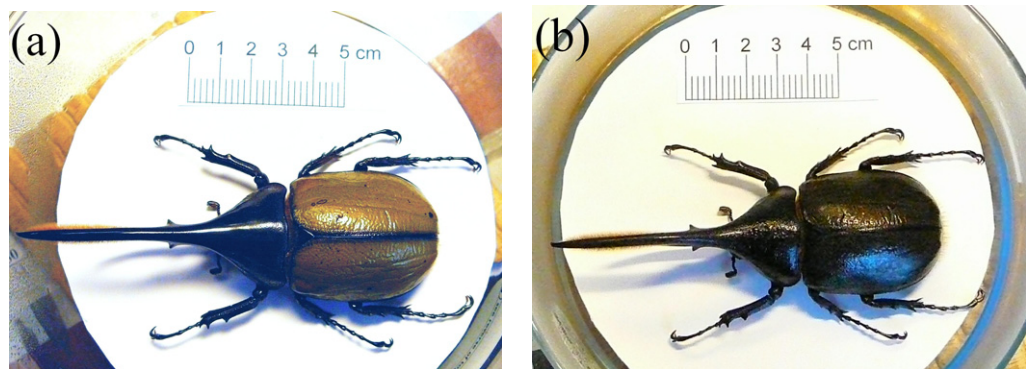


**Figure 3.** (a) The *Dynastes hercules* is greenish with eventually black spots under normal condition of humidity. (b) When put over ebullient water (in order to produce a level of humidity above 80%) the beetle presents a black colouration on all its body.

hypothesis is highly questionable due to the fact that another hercules beetle, the species *Hercules neptunus*, similar in length and morphology to the one studied, shares some repartition area of the *Dynastes hercules* and exhibits a totally black appearance. Because either a green or a black beetle is undetectable in such an environment, the reason for the change of colour might not be related to camouflage.

Another possible function, also proposed by Hinton and Jarman, is thermoregulation. The beetle is still dark when the sun rises, so that it will warm up faster than if green. During the day, the change of colour would prevent the beetle from accumulating heat too fast. This second hypothesis conflicts with two facts. The first is that only the male presents this change of colouration. The female is indeed totally dark except for the apex (i.e. the tip of a wing) of the elytra, but presents nearly the same activity as the male (field observations). The second fact is that this beetle is active during the night and lives in an environment with poor direct



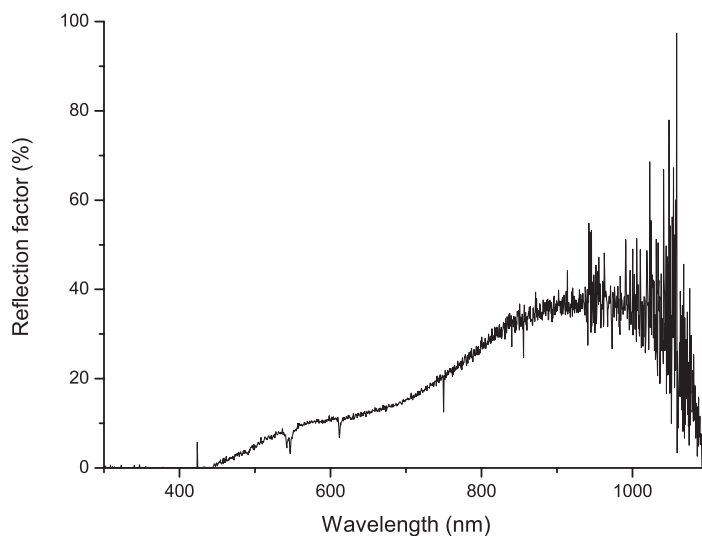


**Figure 4.** Diffusive reflectance spectrum of the cuticle of the *Dynastes hercules*. The curve is taken when the beetle is greenish (humidity level around 40%).

illumination, making the hypothesis of a male specimen basking in the sun unlikely. The reason (if any...) why *Dynastes hercules* has evolved the ability to change colour with humidity is still a mystery which waits to be unveiled.

The aim of the present study is to provide updated data on the morphology of this natural *hygrochromic* structure, to obtain detailed optical data for various humidity states and to re-examine the colouration mechanism with the help of extensive numerical light-scattering simulations. Optical measurements were first carried out with a spectrophotometer in order to quantify the colouration of the beetle in its two reversible states: greenish and black, and at intermediate humidity levels. In parallel, scanning electron microscopy (SEM) was carried out to provide renewed information about the hygrochromic structure, benefiting from imaging improvements brought by thirty years of technology refinement. The modelling part of this work allows us to ensure that the structure seen on SEM images is responsible for the colour observed and reveals the details of the colour selecting mechanism involved.

## 2. Spectral analysis of both states of *Dynastes hercules*

The male specimen used for this study originates from Ecuador and was acquired from an insect collector in Lyon, France. One of the elytra of the beetle (i.e. the hard case that protects the insect's wings) was removed. Part of it was then glued and pressed on a microscope slide, coloured face up, in order to improve the sample flatness. The humidity level was measured with a RS-1360 digital humidity and temperature meter. Spectroscopic measurements were performed using an Avaspec 2048/2 fibre-optic spectrophotometer equipped with an integrating sphere. The sample was illuminated by an unbalanced deuterium-halogen source and the diffuse reflectance spectrum (using the integrating sphere) shown in figure 4 was obtained under a dry atmosphere (40% humidity). The noise at large wavelengths indicates the limited intensity provided there by the halogen source used. The spectrum shows two rather wide components, one centred near 930 nm (beyond the human visible spectrum end, near 700 nm) and the other

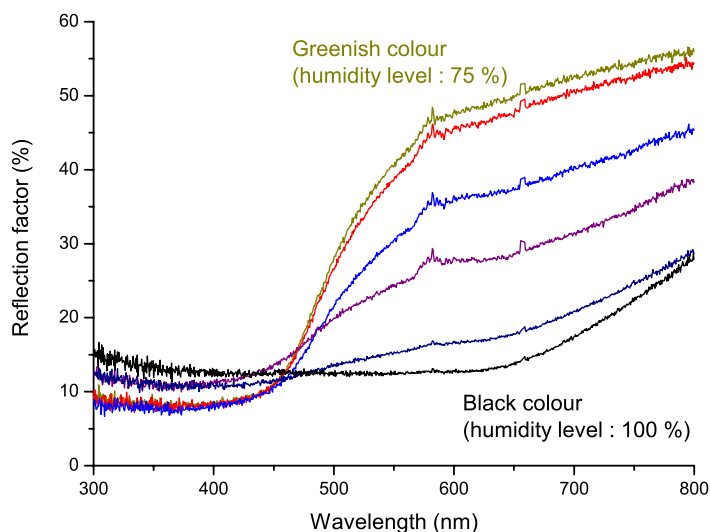


**Figure 5.** Reflectance spectra of the cuticle of *Dynastes hercules*. The curve labelled *Greenish colour* is taken when the beetle is greenish under a humidity level of 75%. The curve labelled *Black colour* is taken when the beetle is totally black under a humidity of 100%. In between, spectra at progressive increasing level of humidity are shown (86, 91, 95 and 97%, respectively).

occurring around 580 nm and extending down to about 420 nm. This second contribution adds a very desaturated yellow-green colour to the non-perceptible red-infrared component. This could explain why the human eye sees a greenish (khaki-green) colour as a result of this spectrally broad scattering.

In order to record the transformation of the elytra from green to black under varying hygroscopic conditions, measurements were performed in a backscattering conformation at normal incidence (i.e. normal to the average surface of the elytra). The reflectance must be limited to a specular geometry because the integrating sphere does not support a high hygrometry level. A bifurcated optic fibre was used both to illuminate the sample and to collect the backscattered light. The slow increase of humidity level was obtained by putting the sample under a large plexiglas box containing a source of ebullient water.

The series of reflectance spectra in figure 5 indicates a decrease of the reflection factor as the humidity level is raised. It also shows that the change is progressive. The curve labelled *Greenish colour* matches the khaki-green colour observed in the dry state and, as the ambient humidity increases, the reflection factor decreases everywhere in the human visible range. It should be noted that the intensity remains high in the infrared part but this does not influence the observed colour. When the environment is saturated with vapour the reflectance spectrum (labelled *Black colour*) shows a much weaker intensity, in agreement with the black appearance of the elytra. Note that the difference in intensity between these spectra and the one presented in figure 4 is due to the modification of the measurement configuration, however the general aspect is conserved (the peak near 930 nm is not visible on these spectra).

The processes are reversible and easy to reproduce: when the humidity level decreases the colour reverts to khaki-green, and the entire cycle can be repeated many times without damaging the elytron structure. Small black patches, however, consistently persist even if the humidity



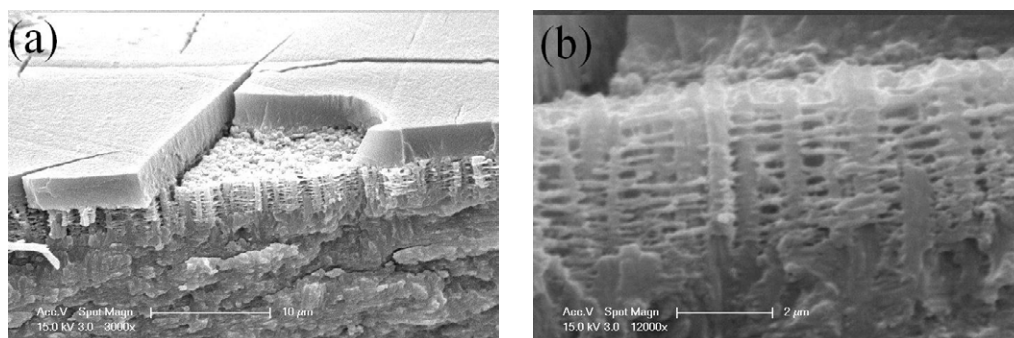


**Figure 6.** Scanning electron micrographs of the cuticle of *Dynastes hercules*. (a) There is an external wax layer with a lot of cracks that allow water to penetrate the structure. This cover is partly removed, allowing the spongy multilayer underneath to be seen. (b) This image allows us to obtain the parameter of the structure for the modelling.

level is low: these permanent black spots have been noticed by entomologists, who describe them as random, their location and even number on the elytra varying on different specimens of the same species. It could be assumed that water is trapped in these spots and cannot evaporate, or—more plausibly—that the colouring structure is highly disturbed.

### 3. Scanning electron microscope images of the cuticle

The other elytron was used to prepare SEM samples. The cuticle (i.e. the external body cover, usually composed of fibrous molecules such as chitin, the most common compound found in insects' exoskeletons) is very hard and immersion in liquid nitrogen allows the sample to be broken with an increased chance of a neat fracture. The images were recorded with a Philips XL20 SEM.

Figure 6(a) reveals a spongy multilayer of some  $3.7 \mu\text{m}$  under a protective wax cover. Note also that the outer part of the cuticle exhibits a number of straight cracks. It is assumed that, in the dry insect, these cracks allow water to penetrate the elytron to wet the multilayer, destroy the scattering strength of its components, and leave a clear view of the black substrate. As the humidity decreases, the water evaporates through the same cracks and the structure returns to its original greenish aspect. Note that the role of the cracks is not so clear with living animals: a specimen of *Dynastes hercules ssp hercules* was kept alive in the laboratory and the external surface of its cuticle seemed hydrophobic enough to make external wetting rather difficult. The living insect did appear completely black in some circumstances, but the exact conditions for the occurrence of the black transformation are still uncertain.

Figure 6(b) indicates that the structure observed is more complex and disordered than a multilayer. The colouring layer is structured as an array of strong vertical columns, perpendicular to the cuticle surface, which supports a layered network of horizontal filaments forming thin permeable plates. The separation between the vertical columns is not much larger than the separation between the horizontal filamentary layers, so that this criss-crossed structure should be classified as a 3D photonic crystal, if the disorder is put aside. The characteristic of this structure is that the empty region is singly connected, as in artificial structures like the

woodpile photonic crystal [27, 28], or in other natural structures like the tree-like shaped ridges of the *Morpho* butterfly [29]. The structure's fully connected empty space will propagate water if the material surface (columns and filaments) is reasonably hydrophilic. The cuticle surface of beetles can be either hydrophobic or hydrophilic, some insects presenting both characters on the same individual [30].

Confirmation that this structure is at the origin of the colouration change is that a strong mechanical stress applied on elytra causes a green region to become black. This suggests that the stress drastically reduces the layer spacing to create an almost continuous medium and this effectively destroys the reflector without any wetting. Unexpectedly, this destruction is sometimes reversible: it has been observed that, when impregnated with water and then left to dry, the green colouration reappears. This experiment has not been subjected to deeper study, but its value as a mechanical memory effect should not be neglected.

The parameters needed to model the optical properties of the structure can be deduced from the SEM images. The material is assumed to be mainly chitin, the basic compound in insects' exoskeletons. The columns, separated by a distance of 610 nm ( $\pm 15$  nm), have an average diameter of 412 nm ( $\pm 5$  nm) and a height of 3.7  $\mu\text{m}$  ( $\pm 0.015$   $\mu\text{m}$ ). There are nearly 10 permeable filamentary slabs with an average thickness of 174 nm ( $\pm 5$  nm). These are separated by hollow gaps with an average width of 197 nm ( $\pm 5$  nm). These parameters will prove useful for estimating the optical response, the subject of the next section.

## 4. Modelling the hygrochromic structure

### 4.1. Simplified model

For a low-index contrast multilayer, as in the present chitin–air structure, the location of the frequency gaps can be predicted, so that the spectral range of the reflectance bands is known [31, 32]. Near normal incidence, a multilayer of period  $a$  develops gaps at wavelengths where the average-index light line meets the Brillouin zone boundaries. These gaps occur at the following wavelengths [18]:

$$\lambda = \frac{2a\bar{n}}{m}, \quad (1)$$

where  $\bar{n}$  is the average refractive index of the structure (to be determined) and  $m$  is an integer chosen so that the reflected wavelength  $\lambda$  lies in the human visible spectrum. The period is easily obtained from the SEM images:  $a = 174 + 197 = 371$  nm, i.e. the sum of the heights of the two kinds of plates (chitin and chitin/air). The average refractive index is less obvious: the precise homogeneization of an optical structure is a difficult problem that has been considered in very recent works [33]. In the present work, due to the irregularity of the structure, we will only produce estimates.

The first step is the evaluation of the refractive index of the chitin/air layers. Considering the proportion of chitin and air in one layer, the dielectric constant  $\varepsilon$  ( $n = \sqrt{\varepsilon}$ ) is given by the average of the perpendicular component:

$$\frac{l}{\varepsilon_{\perp}} = \frac{l_{\text{ch}}}{\varepsilon_{\text{ch}}} + \frac{l_{\text{air}}}{\varepsilon_{\text{air}}}$$

and the parallel one:

$$l\varepsilon_{//} = l_{\text{ch}}\varepsilon_{\text{ch}} + l_{\text{air}}\varepsilon_{\text{air}},$$

where  $\varepsilon_{\text{ch}} = 2.43$  and  $\varepsilon_{\text{air}} = 1.00$ . According to the parameters obtained from the SEM images ( $l_{\text{ch}} = 412$  nm,  $l_{\text{air}} = 610$  nm), the dielectric constant of the chitin/air plates, obtained from an average of the perpendicular and the parallel constants, is found to be equal to  $\varepsilon = 1.445$ .

Using the same formulae, the average refractive index of the whole structure is obtained from the dielectric constants of the chitin and chitin/air plates, with the new parameters (still from the SEM images)  $l_{\text{ch}} = 174$  nm for the chitin plates' height and  $l_{\text{air}} = 197$  nm for the chitin/air plates' height. The constant is  $\overline{\varepsilon_{\text{ch}}} = 1.845$  and so the refractive index is equal to  $\overline{n_{\text{ch}}} = 1.36$ .

With these parameters, equation (1) can be applied to the structure of *Dynastes hercules*. With  $m = 1$ , the dominant reflected wavelength is  $\lambda = 1009$  nm, which is beyond the human visible spectrum and is consistent with the experimental infrared structure observed near 930 nm in figure 4. With  $m = 2$ , the wavelength is  $\lambda = 504$  nm, which can explain the broad structure near 580 nm which develops in the hemispheric reflectance. The agreement is not perfect, but our model is highly idealized.

This simplified model shows its limitations when the spectrum of figure 4 is considered. In particular, equation (1) does not account for the lateral variation of the refractive index, due to the presence of the array of columns that reduces the translational invariance. If we assume that this corrugation is periodic, the component of the incident wavevector parallel to the cuticle surface is not strictly conserved: a 2D lattice vector of length  $g$  can be added as the wave propagates in the colouring layer. When this is taken into account, equation (1) is modified as follows:

$$\lambda = \frac{2a\overline{n}}{\sqrt{m^2 + (ag/\pi)^2}}. \quad (2)$$

This includes the reflection predicted by equation (1), for  $g = 0$ , but also reflections at shorter wavelengths, when  $g \neq 0$ . The effect of the lateral refractive index variation is then primarily to distribute the reflectance on the blue side of the reflection band predicted by the planar homogeneous layer model. In the present case, since the lateral index corrugation is not periodic, the lattice parameter must be considered to be very large, and the reciprocal lattice vectors are built on a reciprocal unit cell which is very small, compared to the vertical lattice spacing  $a$ . This means that the added reflections associated with the infrared  $m = 1$  form a continuous sideband extending towards the blue, possibly accounting for the asymmetric lineshape observed in figures 4 and 5.

In the next section, we bring a confirmation of this analysis from an independent point of view, based on the calculation of the response of a full 3D model.

#### 4.2. Optical response of a 3D model structure

By solving Maxwell's equations, the reflectance spectra of a photonic-crystal film can be obtained. The most direct approach is the transfer–matrix method [34, 35], which takes full account of the multiple scattering in 3D and describes the ingoing and outgoing light as simple plane waves with precise propagating direction and polarization.

The model (see figure 7) is constructed with parameters determined from SEM images. It is formed of columns of chitin, related to each other by thin bars, also made of chitin. The structure contains a singly connected network of pores, to be as close as possible to the observed structure.

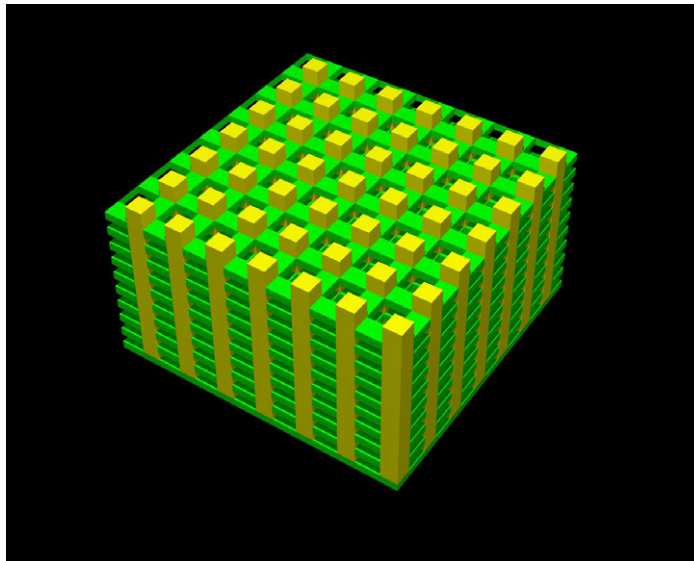


**Figure 7.** Model of the structure producing the colour of the elytra of *Dynastes hercules*. The porous structure is formed of chitin piles linked to each other by chitin chains.

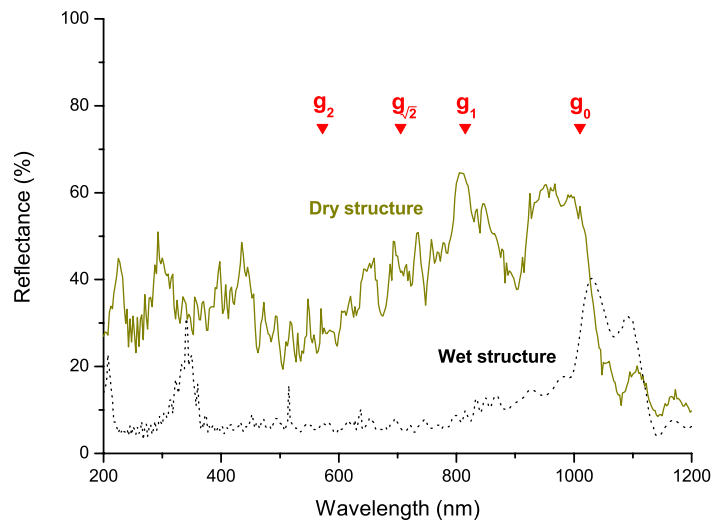
Since no iridescence is observed in the measured sample, the reflection must be insensitive to the incidence and emerging angles, as well as any azimuthal variation of the illumination and viewing angles. We then calculate the hemispheric reflectance, and average over all possible polar and azimuthal incidence directions. The loss of significance of the incidence and emerging directions is related to the strong disorder exhibited by the real structure, and the presence of a thick diffusive layer covering the colouring structure. This cover layer is represented in our model by a planar  $3\ \mu\text{m}$  thick clear slab, but the averaging over the propagation directions will replace the diffusive properties.

Figure 8 shows theoretical spectra produced by the model. The first curve labelled *Dry structure* corresponds to the dry porous structure. The strong reflection band around 980 nm found in figure 4 is recovered. The sideband, due to the lateral corrugation is also present, extending from 900 nm to about 500 nm. For the square lattice used in the present model, the lengths of the shortest reciprocal lattice vectors are given by  $g = \eta(2\pi/b)$ , where  $b = 1022\ \text{nm}$  is the lateral square-lattice parameter, and

$$\eta = 0, 1, \sqrt{2}, 2, \sqrt{5}, \dots$$

The 3D reflectance calculation shows that the infrared gap and its sideband essentially contains contributions from the reciprocal lattice vectors  $g_0, g_1, g_{\sqrt{2}}$  and  $g_2$  which are predicted by equation (2) to lie respectively, at  $\lambda = 1009, 816, 704$  and  $572\ \text{nm}$ . The decrease of the sideband towards the blue, down to about 500 nm, agrees well with the observation but the ordered model exaggerates the contributions of higher gaps, in the blue and ultraviolet. In spite of these discrepancies, the physical origin of the dry-state colouration of the insect as a 3D photonic-crystal effect is clear.

The other curve, labelled *Wet structure* is calculated from the same 3D structure, but the empty spaces are now filled with water (refractive index 1.33). One can immediately note the drastic fall of intensity in the whole human visible spectrum, producing the black colour



**Figure 8.** Theoretical reflectance spectra of the structure studied. The solid curve labelled *Dry structure* corresponds to the dry porous structure. The dotted curve labelled *Wet structure* corresponds to the same structure filled with water. The predicted values of the reciprocal lattice vectors are shown.

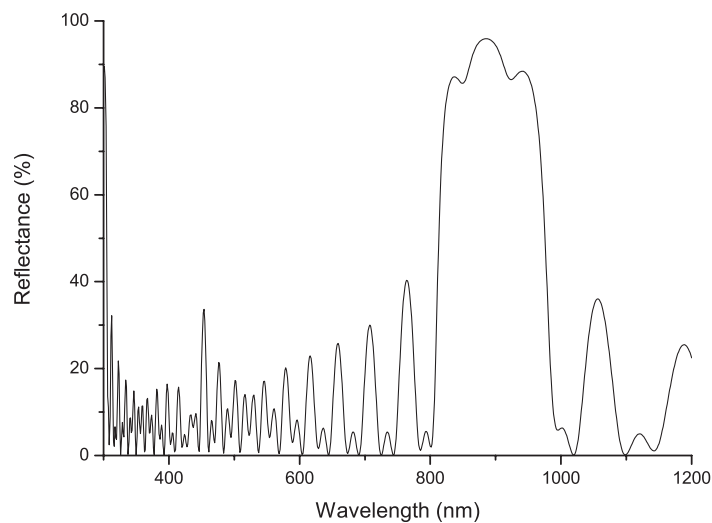


**Figure 9.** Theoretical reflectance spectrum of the structure studied assimilated to a simple multilayer.

observed on the elytra under the high humidity level. All air/chitin interfaces in the model become water/chitin interfaces, with a local normal reflectance that drop from 4.7 to 0.6%, explaining the fact that the photonic-crystal structure loses the multiple scattering power which allows the formation of gaps. The structure then becomes clear, leaving a free path for the transmission of light to the absorbing substrate.

Figure 9 shows a spectrum for an ideal planar multilayer with parameters (layer thicknesses and refractive indices) consistent with our 3D model. There are no more chitin columns nor filamentary plates, but the two kinds of homogeneous plates with effective refractive indices alternate. The experimental band near 930 nm is retrieved, but the sideband is absent. The



consequence is that no contribution to the reflectance appears in the human visible spectrum, except for Fabry-Pérot resonances, due to the presence of sharp interfaces between the colouring film boundaries. This emphasizes that, in contrast to many other natural photonic crystals, the present structure colouration cannot be explained without the 3D structure inducing the sideband of the infrared gap. Many 3D structures exist in nature, but many of them—on Lepidoptera like *Polyommatus daphnis* or Coleoptera like *Hoplia coerulea*—produce zero-order lateral lattices that do not provide the sideband described in the present work. The present optical device is then of particular interest, even if its hygrochromic behaviour is neglected.

## 5. Conclusion

The change of colour of the *Dynastes hercules* under varying humidity is due to the penetration of water into a 3D porous structure, attenuating the contrast of refractive index and leaving a view of the pigmented absorbing substrate. This effect was observed and discussed several years ago [17], but the present paper addresses the reverse engineering of this complex system in a more complete way and clarifies several aspects of this hygrochromic effect.

The current knowledge of this system was supplemented by new, higher-resolution, SEM images and by optical reflectance measurements. The physical analysis of this structure, assisted by numerical simulations, has shown that the structure cannot be assimilated to a simple 1D multilayer, but that its understanding requires a fully 3D treatment. This seems to be rather exceptional: 3D-photonic crystals found in nature (among those studied by the authors) can be viewed, in a first approach, as 1D multilayers. In the present case, reducing the structure to a multilayer leads to the complete loss of the khaki-green colouration displayed by the beetle.

Hygrochromic behaviour could be an important property of an ‘intelligent’ material. Such materials could be put to work as humidity sensors, perceptibly changing colour according to the hygrometry level. This could be useful for example in food processing plants to monitor the moisture level. Since optical properties can be transferred to other radiative spectral ranges by scaling the structure lengths up or down, hygrochromic materials could also find thermal uses. Microporous materials, such as natural zeolites, have been used as building blocks [36], with the added benefit of temperature stabilization.

## Acknowledgments

This work was carried out with the support from EU5 Centre of Excellence ICAI-CT-2000-70029 and from the Inter-University Attraction Pole (IUAP P5/1) on ‘Quantum-size effects in nanostructured materials’ of the Belgian Office for Scientific, Technical, and Cultural Affairs. We acknowledge the use of the Namur Interuniversity Scientific Computing Facility (Namur-ISCF), a common project between the Belgian Fund for Scientific Research (FRS), and the Facultés Universitaires Notre-Dame de la Paix (FUNDP, University of Namur). This work has been partly supported by the European Regional Development Fund (ERDF) and the Walloon Regional Government under the ‘PREMIO’ INTERREG IIIa project.

We gratefully thank the Museum of Besançon and especially Jean-Yves Robert (Curateur collections zoologiques) for providing information during this study and the donation of a living and captive born specimen of *Dynastes hercules* ssp *hercules*. We also acknowledge Fortuné Chalumeau (Institut de Recherches Entomologiques de la Caraïbe) for much information about



the lifestyle of *Dynastes hercules* and Dr Ir Olivier Deparis (Laboratoire de Physique du Solide, University of Namur) for a helpful critical reading.

M R was supported as PhD student by the Belgian Fund for Industrial and Agricultural Research (FRIA). J F C was supported by the Belgian Fund for Scientific Research (FRS).

## Appendix

In this appendix, we give a brief justification of equation (2), which is fundamental to the present analysis. We consider a semi-infinite photonic-crystal film with a ‘vertical’ periodicity  $a$  (in the direction normal to its surface, set to the  $z$ -direction). The lateral (parallel to the surface) periodicity is given by the 2D lattice vectors  $\vec{a}_1$  and  $\vec{a}_2$ , which generate the reciprocal lattice vectors  $\vec{g}$ . We consider the case where the incident light falls along the normal, so that its wavevector has no lateral component. The wavevector inside the material has a normal component  $k_z$  and, due to diffraction by the lateral periodic structure, a lateral component  $\vec{k}_\parallel = \vec{g}$ .

As the wave angular frequency  $\omega$  is conserved, the norm of the effective wavevector in the photonic crystal is given by

$$|k|^2 = k_z^2 + k_\parallel^2 = \bar{n}^2 \frac{\omega^2}{c^2},$$

where  $\bar{n}$  is the average refractive index of the whole structure. The condition for the opening of a gap in the backscatter ( $z$ ) direction is that the ‘vertical’ wavevector lies at the boundary of one of the extended-scheme Brillouin zones, at

$$k_z = m \frac{\pi}{a},$$

where  $a$  is the period of the photonic crystal normal to its surface. Putting this together gives us

$$\bar{n}^2 \frac{\omega^2}{c^2} = m^2 \frac{\pi^2}{a^2} + g^2.$$

It follows immediately that

$$\lambda = \frac{2\pi c}{\omega} = \frac{2a\bar{n}}{\sqrt{m^2 + (ag/\pi)^2}}.$$

## References

- [1] Michelson A A 1911 On metallic colouring in birds and insects *Phil. Mag.* **21** 554
- [2] Rayleigh Lord 1918 On the optical character of some brilliant animal colours *Phil. Mag.* **37** 98–111
- [3] Rayleigh Lord 1923 Studies of iridescent colour, and the structure producing it. IV Iridescent beetles *R. Soc. Proc. A* **103** 233
- [4] Bancroft W D, Chamot E M, Merritt E and Mason C W 1923 Blue feathers *The Auk* **40** 275–300
- [5] Mason C W 1927 Structural colors in insects II *J. Phys. Chem.* **31** 321
- [6] Gentil K 1942 Elektronenmikroskopische Unetersuchung des Feinbaues schillernder Leisten von Morpho-Schuppen *Z. Morph. Okol. Tiere* **38** 344
- [7] Taylor R L 1964 The metallic gold spots on the pupa of the monarch butterfly *Ent. News* **75** 253
- [8] Nekrutenko Y P 1965 Gynandromorphic effect and the optical nature of hidden wing-pattern in *Gonepteryx rhamni* L. (Lepidoptera, Pieridae) *Nature* **205** 417

- [9] Land M F 1966 A multilayer interference reflector in the eye of the scallop *J. Exp. Biol.* **45** 433
- [10] Bernhard C G, Gemne G and Moeller A R 1968 Modification of specular reflexion and light transmission by biological surface structures *Q. Rev. Biophys.* **1** 89–105
- [11] Neville A C and Caveney S 1969 Scarabaeid beetle exocuticle as an optical analogue of cholesteric liquid crystals *Biol. Rev.* **44** 531
- [12] Vukusic P and Sambles J R 2003 Photonic structures in biology *Nature* **424** 852–5
- [13] Parker A 2000 515 Million years of structural colour *J. Opt. A* **2** 15–28
- [14] Yin H, Shi L, Sha J, Li Y, Qin Y, Dong B, Meyer S, Liu X, Zhao L and Zi J 2006 Iridescence in the neck feathers of domestic pigeons *Phys. Rev. E* **74** 051916
- [15] Prum R O and Torres R H 2004 Structural colouration of mammalian skin: convergent evolution of coherently scattering dermal collagen arrays *J. Exp. Biol.* **207** 2157–72
- [16] Parker A R and Townley H E 2007 Biomimetics of photonic nanostructures *Nat. Nanotechnol.* **2** 347–53
- [17] Hinton H and Jarman G 1972 Physiological colour change in the Hercules beetle *Nature* **238** 160–1
- [18] Vigneron J P, Rassart M, Vandembem C, Lousse V, Deparis O, Biró L P, Dedouaire D, Cornet A and Defrance P 2006 Spectral filtering of visible light by the cuticle of metallic woodboring beetles and microfabrication of a matching bioinspired material *Phys. Rev. E* **73** 041905
- [19] Vigneron J P, Colomer J F, Vigneron N and Lousse V 2005 Natural layer-by-layer photonic structure in the squamae of *Hoplia coerulea* (Coleoptera) *Phys. Rev. E* **72** 061904
- [20] Deparis O, Vandembem C, Rassart M, Welch V L and Vigneron J P 2006 Color-selecting reflectors inspired from biological periodic multilayer structures *Opt. Express* **14** 3555
- [21] Kertész K, Bálint Z, Vértesy Z, Márk G, Lousse V, Vigneron J P, Rassart M and Biró L 2006 Gleaming and dull surface textures from photonic-crystal-type nanostructures in the butterfly *Cyanophrys remus* *Phys. Rev. E* **74** 021922
- [22] Lachaume G 1985 *The Beetles of the World* vol 5 *Dynastini* (Venetier, France: Sciences Nat)
- [23] Chalumeau F 1999 *Dynastes hercules hercules* Linné: approches faunistiques (en son milieu de la forêt mésophile de Guadeloupe) et un modèle théorique relatif à son éthologie (Coleoptera, Scarabaeidae) *Nouv. Revue Ent.* **16–4** 365–72
- [24] Chalumeau F and Reid W 2002 Aperçus sur le complexe *hercules* et statut du *Dynastes alcides* (Coleoptera, Dynastidae) *Nouv. Revue Ent.* **19–1** 83–91
- [25] Vigneron J P *et al* 2007 Switchable reflector in the Panamanian tortoise beetle *Charidotella egregia* (Chrysomelidae: Cassidinae) *Phys. Rev. E* **76** 031907
- [26] Hinton H and Jarman G 1973 Physiological colour changes in the elytra of the Hercules beetles, *Dynastes hercules* *J. Insect Physiol.* **19** 533–49
- [27] Ho K M, Chan C T, Soukoulis C M, Biswas R and Sigalas M 1994 Photonic band gaps in three dimensions: new layer-by-layer periodic structures *Solid State Commun.* **89** 413–6
- [28] Noda S, Yamamoto N, Kobayashi H, Okano M and Tomoda K 1999 Optical properties of three-dimensional photonic crystals based on III-V semiconductors at infrared to near-infrared wavelengths *Appl. Phys. Lett.* **75** 905–7
- [29] Vukusic P, Sambles J, Lawrence C and Wootton R 1999 Quantified interference and diffraction in single Morpho butterfly scales *Proc. R. Soc. Lond. B: Biol. Sci.* **266** 1403–11
- [30] Parker A and Lawrence C 2001 Water capture from desert fogs by a Namibian beetle *Nature* **414** 33–4
- [31] Joannopoulos J, Meade R and Winn J 1997 *Photonic Crystals* (Princeton, NJ: Princeton)
- [32] Inoue K and Ohtaka K 2004 *Photonic Crystals* (Berlin: Springer)
- [33] Guenneau S and Zolla F 2007 Homogenization of 3D finite chiral photonic crystals *Physica B* **394** 145–7
- [34] Pendry J B and MacKinnon A 1992 Calculation of photon dispersion relations *Phys. Rev. Lett.* **69** 2772–5
- [35] Vigneron J P and Lousse V 2006 Variation of a photonic crystal color with the Miller indices of the exposed surface *Proc. SPIE* **6128** 325–34
- [36] Mumpton F A 1999 La roca magica: Uses of natural zeolites in agriculture and industry *Proc. Natl Acad. Sci. USA* **96** 3463–70